# High-throughput gated photon counter with two detection windows programmable down to 70 ps width

Gianluca Boso,[1] Alberto Tosi,[1,a)] Alberto Dalla Mora,[2] and Franco Zappa[1]
[1]*Dipartimento di Elettronica, Informazione e Bioingegneria, Politecnico di Milano, Piazza Leonardo Da Vinci 32, 20133 Milano, Italy*
[2]*Dipartimento di Fisica, Politecnico di Milano, Piazza Leonardo Da Vinci 32, 20133 Milano, Italy*

(Received 30 August 2013; accepted 31 December 2013; published online 21 January 2014)

We present the design and characterization of a high-throughput gated photon counter able to count electrical pulses occurring within two well-defined and programmable detection windows. We extensively characterized and validated this instrument up to 100 Mcounts/s and with detection window width down to 70 ps. This instrument is suitable for many applications and proves to be a cost-effective and compact alternative to time-correlated single-photon counting equipment, thanks to its easy configurability, user-friendly interface, and fully adjustable settings via a Universal Serial Bus (USB) link to a remote computer. © *2014 AIP Publishing LLC*. [http://dx.doi.org/10.1063/1.4862060]

## I. INTRODUCTION

Nowadays an increasing number of applications in different research and industrial fields need to detect light signals at single-photon level with high timing accuracy (down to few tens of picoseconds) and high throughput (tens of millions of events per second). Just to mention a few: fluorescence lifetime imaging (FLIM),[1,2] Förster resonance energy transfer (FRET),[3,4] fluorescence correlation spectroscopy (FCS),[5] functional brain imaging,[6] optical mammography,[7] molecular imaging,[8] quantum information, and many others. Most of these applications make use of the time-correlated single-photon counting (TCSPC) technique to reconstruct the optical waveform of the signal of interest in the time domain.[9] This technique consists of the use of a picosecond pulsed laser as excitation source, a single-photon detector (e.g., single-photon avalanche diode, photomultiplier tube, superconducting single-photon detector, etc.) to signal each photon event (count) produced by the object under investigation and a timing instrument (like a time-to-digital converter or a time-to-amplitude converter) to mark the arrival time of every such event.

The histogram of the arrival time for every photon represents the probability distribution function of the photon in time and hence corresponds to the intensity of the light signal to be reconstructed, provided that the probability to detect a photon per excitation cycle is much less than one.[9] The information to be acquired is usually encoded in one or more properties of the reconstructed optical waveform (i.e., the TCSPC histogram), like its peak amplitude, the overall number of collected photons or the exponential life-time constant for decaying signals. These parameters can be extracted from the TCSPC histogram in post-processing.

The TCSPC technique provides the user with an information-rich data set, e.g., the time-dependent waveform for every time-bin of the reconstructing timing instrumentation. Very often only a much-reduced portion of data is necessary to extract the main parameters of interest (e.g., the time constant of the decay curve in fluorescence imaging or the number of counts occurring within a well-defined time window in functional near infrared spectroscopy[10]). On the other hand, in order to provide picosecond resolution, the TCSPC timing instrumentation is usually complex, expensive, and with a not-negligible conversion time (i.e., the time needed to compute the arrival time of a single event), which limits the maximum acquisition rate of the overall detection system. These limitations drastically restrict the effective exploitation of classical TCSPC techniques to systems with only few detection channels and with limited throughput, up to few mega counts per second (cps).[11–14]

The urge to employ single-photon acquisition chains with throughput up to hundreds of Mcps has recently led to the development of novel detection systems based on multiplexed techniques,[15] sinusoidal gating of Single-Photon Avalanche Diodes (SPADs),[16–18] or cryogenic detectors capable of such high count rates.[19] Unfortunately neither commercial nor research TCSPC products are yet capable of handling such high throughputs.

Gated photon counters have been proposed as an alternative to TCSCP systems to extract timing information from single-photon detectors both as commercial[20,21] and research products.[22,23] These instruments, once interfaced with a single-photon detector, can count the impinging photon events only during one or more well-defined counting windows, synchronized with the excitation laser and whose duration can be programmed down to few nanoseconds or hundreds of picoseconds. By placing the counting windows in the appropriate time-delay position with respect to the waveform to be acquired, various curve parameters can be extracted. The state-of-the-art for such instruments withstands count rates from few tens of millions to hundreds of millions of counts per second, but provides detection windows with widths of more than 500 ps, thus inhibiting their exploitability with fast decaying signals (e.g., with life-times shorter than 1 ns) or when the technique requires the acquisition of the integral counts in a very short (<500 ps) time interval of the curve.

a)E-mail: alberto.tosi@polimi.it

 

Here we present the design and characterization of a novel high-throughput gated photon counter with two programmable very short counting windows. Thanks to the use of fast discrete logic elements and since this module does not rely on the precise reconstruction of every photon arrival time, there is no conversion time overhead and the throughput can be increased up to 100 Mcps while keeping the flexibility of two programmable windows with widths from 10 ns down to 70 ps. Furthermore, the proposed solution can be easily parallelized for both discrete and integrated architectures, thus enabling multichannel single-photon detection systems in many yet unexplored applications.

This paper is organized as follows: Sec. II deals with the design of the developed gated counter, whose experimental characterization is presented in Sec. III. Finally, Sec. IV summarizes the work.

## II. GATED PHOTON COUNTER DESIGN

### A. Gated counting principle

Figure 1(a) shows a typical photon counting setup. The sample under test, excited by a picosecond pulsed laser source, emits light (see the optical waveform of Fig. 1(b)). Many times the response has an exponential decay, which contains the information to be extracted, e.g., the time constant of the fluorophore or the scattering and absorption coefficients of the diffusive material. The optical signal emitted by the sample is faint (down to single-photon level) and fast (with picosecond or sub-nanosecond transitions), hence a single-photon detector like a SPAD[24] can be used to acquire the waveform. A photon counting board, synchronized with the laser pulse excitation (START signal) collects the time delay (sometimes called the Time-of-Flight (TOF) in LIDAR applications) of the electrical pulses provided by the single-photon detector (STOP signal). In case of a TCSPC board, the time delay between START and STOP pulses is computed for every collected photon and a histogram of the arrival times is plotted (Fig. 1(c)). This histogram represents the shape of the optical waveform with picosecond resolution, depending on the given time bin of the employed TCSPC board.

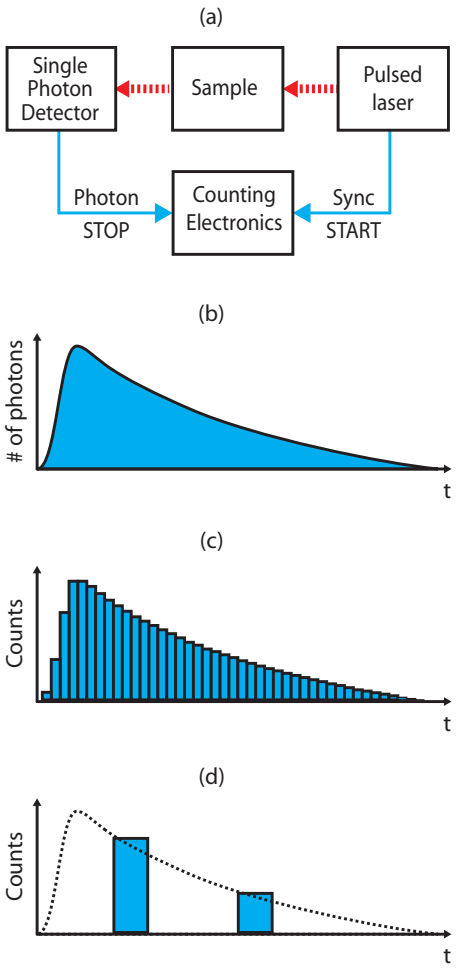


FIG. 1. Gated counting principle. (a) Typical photon counting setup where a TCSPC board collects time delays between the excitation sync signal and the arrival time of each detected photon, and reconstructs the optical waveform through the cumulative histogram of repetitive events. (b) Example of an optical waveform to be reconstructed. (c) TCSPC reconstruction. (d) Two-point gated counting acquisition of the same optical waveform.

If the shape of the waveform is known *a priori* (e.g., it is a single-exponential decaying curve), a particular property of the waveform can be extracted by using just few samples of the entire histogram. For example, the life-time constant of a fluorophore can be computed by acquiring two samples on the fluorescence curve or, in time-resolved functional near infrared spectroscopy, the changes in the absorption and scattering coefficient (hence in the concentration of hemoglobin) can be computed by integrating the photons of the reflectance curve in a defined time window (<500 ps) to monitor a specific region of the biological tissue under test.[7,8]

In order to do so, a gated counter can be used instead of a TCSCP board. In fact, Fig. 1(d) shows the same curve acquired with a two-window gated counter. Only photons impinging onto the detector in those two well-defined time-intervals (gates) are collected and can be used to extract the desired parameter. To be able to acquire these two time samples, we implemented two separate timing chains with user-selectable time-delays. In this way, the temporal position of the gates can be moved in time over the entire range of interest of the waveform (see Fig. 1(d)).

### B. Block diagram

Figure 2 shows the block diagram of the gated counter module, consisting of fast Emitter-Coupled Logic (ECL) components for the input stage and the two counting windows, a Complex Programmable Logic Device (CPLD) and a microcontroller to provide both a reconfigurable counter and a timer, and to manage the functionalities of the whole module, including the USB link for parameter setting and data uploading to a remote computer.

The module has two SubMiniature version A (SMA) inputs: PHOTON IN and SYNC. SYNC must be connected to a synchronization signal (usually a laser trigger-out signal) and is used as time reference to generate the two counting windows. PHOTON IN must be connected to the pulse stream to be acquired and counted. As said before, the pulse stream could be generated by a single-photon detector that provides one electrical output pulse coincident with the arrival time of each detected photon.

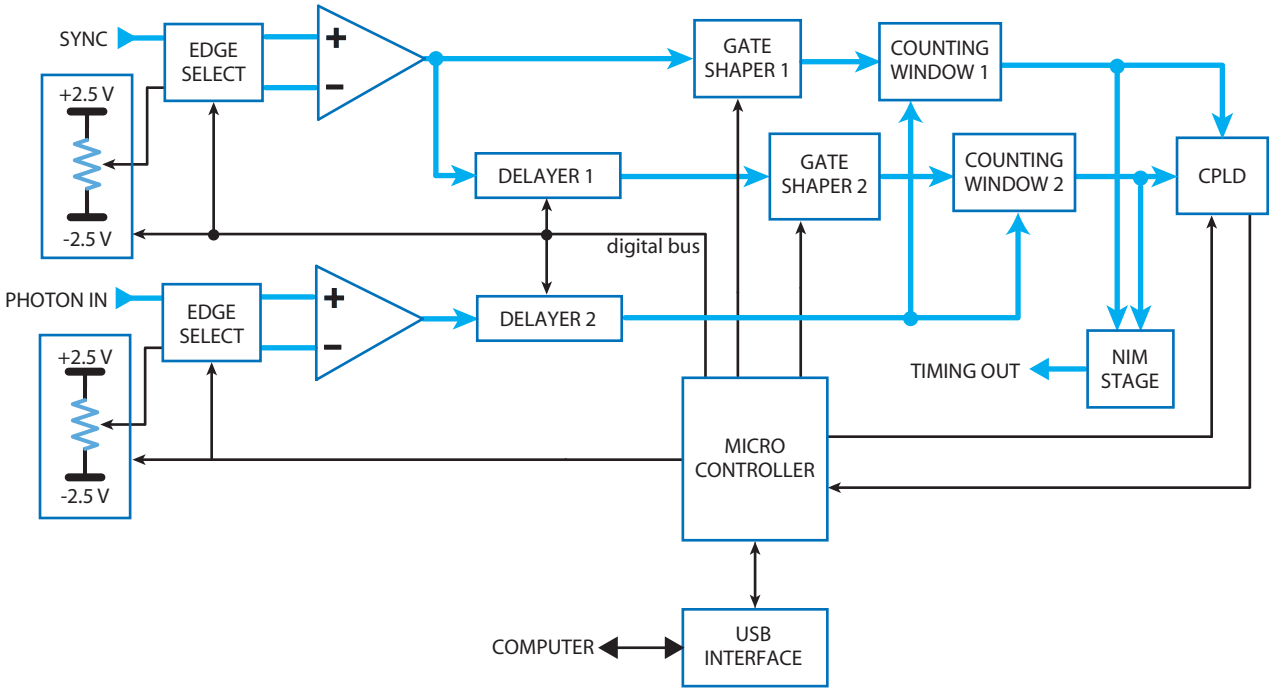


FIG. 2. Block diagram of the gated counter. Two input stages generate two distinct digital outputs synchronized with the rising or falling edges (user-selectable) of the SYNC and PHOTON IN signals. The PHOTON IN signal can be delayed via a user-controllable delay line (DELAYER 2), while the SYNC signal is used to generate two distinct gate windows whose relative position in time can be adjusted via DELAYER 1. Two counting windows count only PHOTON IN pulses arriving within the two specified windows. A CPLD and a microcontroller are used to read-out the counts and provide a simple user interface through a USB connection.

The two input stages are identical for both signals and consist of an RF double-pole double-throw (DPDT) relay with 8 GHz analog bandwidth, a fast ECL comparator (AD-CMP582, Analog Devices) with 12.5 Gbps toggle rate and an ECL monostable (based on NBSG53A, On Semiconductors). By selecting the appropriate configuration of the relay via the microcontroller, each input can be connected to either the positive or negative terminal of the ECL comparator and hence be configured to be sensitive on either the rising or falling edge of the respective signal. The comparator has a user selectable threshold that spans from −2.5 V to +2.5 V with 10-bit resolution, corresponding to approximately 5 mV steps. In order to correctly process every pulse, the output of the comparator feeds a monostable to generate standard pulses with 3 ns fixed duration.

After the input stages, two programmable ECL delayers (MC100EP196, On Semiconductors) are used to select the temporal shift of the two counting windows with respect to each other (DELAYER 1) and the shift between the SYNC and the PHOTON IN signals (DELAYER 2). Hence, DELAYER 2 is used to place the waveform in the correct time position with respect to the first window (see Fig. 1(d)) while DELAYER 1 is used to move the second window with respect to the position of the first one. The delay lines have 10 ps resolution and 10 ns delay range. In this way, the two counting windows can be precisely placed in any time position within a range from 0 ns to 10 ns with respect to the optical waveform to be acquired.

After the delay lines, two gate shapers are used to independently select the duration of the two counting windows. The duration of the SHAPER OUT pulses can be set in a wide range between 70 ps and 10 ns, with 10 ps steps.

Two fast ECL flip-flops (NBSG53A, On Semiconductors) implement the counting windows themselves. They receive the delayed PHOTON IN signal to be acquired, the gate durations and their time positions from the gate shaping stages. Only the PHOTON IN pulses that are falling within the desired time (gate) interval are counted; all the others are discarded with picosecond precision.

The outputs of the two counting windows can be routed to a CPLD (EPM240, Max II Series, Altera) where two programmable 32-bit counters are implemented or, as an alternative, they can be routed to an output stage to be processed by external instrumentation (e.g., a TCSPC board for testing purposes or an external counter).

The CPLD contains two separate 32-bit counters capable of a maximum count rate of 100 MHz each and a programmable 18-bit timer with 10 ms resolution to implement the integration time duration of the counters, up to approximately 40 min.

An 8-bit microcontroller is installed on board to set all programmable parameters (input thresholds, delays, gate window durations, integration time) and to read-out the values from the 32-bit counters. The microcontroller is equipped with a USB 2.0 interface for bi-directional communication with a remote computer.

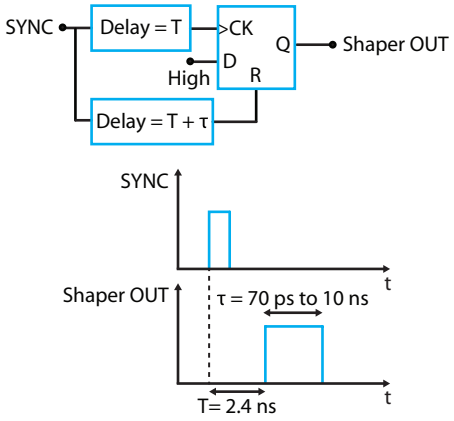


FIG. 3. Gate shaper. The duration (width, $\tau$) of the counting window is selected by changing the value of a finely adjustable delay line (from 70 ps up to 10 ns). A second delay line is added to compensate for the intrinsic delay (T = 2.4 ns) of the first one. The propagation delay of the flip-flop is not represented.

In Secs. II C–II E, each of the main elements of the instrument is analyzed in detail.

### C. Generation of the window width

Figure 3 shows the schematic of one of the two gate shapers implemented in the gated photon counter. The function of each gate shaper is to define and output a logic (ECL level) pulse with programmable duration, hence representing the counting windows that will later select the photons to be counted.

The gate shaper is implemented with an ECL D-type flip-flop with asynchronous reset (NBSG53A, On Semiconductors). The D input is kept at logic level ''1,'' while the CLOCK and the RESET inputs are fed by a delayed version of the SYNC input signal. The output SHAPER OUT is initially at logic level ''0'' and switches to ''1'' at the rising edge of the CLOCK signal, just to switch back to ''0'' at the rising edge of the RESET signal. In this way, the duration ($\tau$) of SHAPER OUT is set by the time delay difference between CLOCK and RESET, which can be finely tuned with 10 ps steps, from 70 ps to 10 ns. The gate shaper employs two delay lines in order to compensate their intrinsic T = 2.4 ns delay, which otherwise will result as the minimum gate width. In this configuration, instead, the minimum gate window is limited by the minimum output pulse width obtainable by the ECL flip flop. By using a fast SiGe ECL flip-flop with 35 ps transition times (20%–80%), a 70 ps Full-Width at Half Maximum (FWHM) pulse width is achievable.

### D. Counting window and output stage

Figure 4 shows the schematics of one of the two counting windows implemented in the gated photon counter. The function of the counting window is to selectively count only pulses falling within such window.

The counting window is implemented by using the same fast SiGe ECL D-type flip-flop with asynchronous reset used for the gate shaper: the delayed PHOTON IN pulses are applied to the CLOCK input, whilst the SHAPER OUT signal is

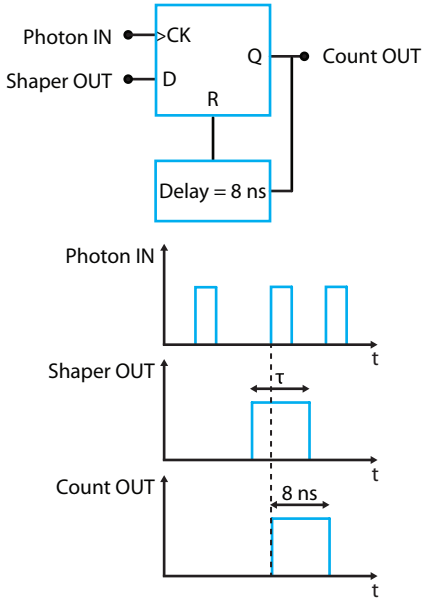


FIG. 4. Counting window. The PHOTON IN stream to be acquired is applied to the clock input of a fast ECL D-type flip-flop. The D input implements the gating function: when SHAPER OUT is at logic level HIGH, the flip-flop output Q is set HIGH by the clock signal. A delay line between Q and R sets the duration of the output pulse to 8 ns.

applied to the D input. In this configuration only the CLOCK transitions falling within the gate window (i.e., when D is set to logic level ''1'') results in a transition of the Q output (COUNT OUT), otherwise they are ignored.

The Q output (COUNT OUT) is connected to the asynchronous RESET input through an 8 ns delay line. In this way, the flip-flop output pulse is set with a fixed duration of 8 ns, compatible with the minimum pulse width requirements for the following CPLD input stage.

The output pulses from each of the two counting windows are routed through a multiplexer to either the CPLD or the output stage. The latter provides NIM (Nuclear Instrumentation Modules) output pulses from 0 V to −0.8 V, compatible with most of the commercial TCSPC boards. This additional output can be used to characterize the performance of the gating windows or it can be exploited to connect the gating part of the instrument to an external counter or TCSPC board.

### E. Programmable counter and timer

Figure 5 shows the schematics of the two logic blocks implemented inside the CPLD (EPM240, Max II Series, Altera). Figure 5(a) shows the implementation of a 32-bit counter. A first counting block is enabled for a well-defined integration time through the CK_ENABLE pin, by the onboard microcontroller, and detects all COUNT OUT pulses from the corresponding gating window (CK input). The resulting number of counts is stored into an array (q[0:31] bus), which is read by the microcontroller through a serial interface and a shift register.

Figure 5(b) shows the schematics of the programmable timer, which sets the integration time for the two counters within the CPLD. The time base is an external 4 MHz oscillator with an overall frequency stability of 25 ppm, from

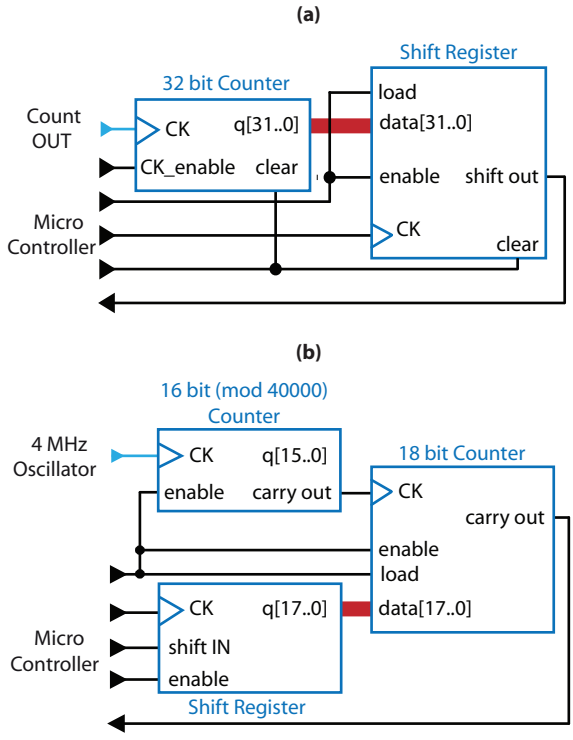


FIG. 5. (a) Schematics of the counter block implemented inside the CPLD. The programmable chip contains two counter blocks, one for each gating window. (b) Schematics of the timer block. A stable crystal oscillator is used as a reference and is divided by 40 000 in order to obtain a 100 Hz time base. Both counters and the timer can be configured by the user via the microcontroller and its USB link.

−10 °C to +70 °C. Such time base is then divided by a fixed modulus-40000 counter to obtain a very stable 100 Hz time base. Another 18-bit serially programmable counter receives the 100 Hz reference and outputs a synchronization signal, which spans from 10 ms to approximately 40 min, user-selectable through the microcontroller interface, and is used to enforce the integration time of the instrument.

## III. EXPERIMENTAL CHARACTERIZATION

All previously described building blocks are assembled in a 4-layer printed circuit board (PCB). Another custom-made board houses the power supply unit that provides all power rails for the correct operation of all components starting from the standard 110 V/220 V mains. Everything is housed within an aluminum box (23 cm × 23 cm × 8 cm) to provide adequate temperature stabilization through a copper heat sink (connecting the bottom of the PCB to the housing) and a fan.

We performed an extensive characterization of the module in terms of temporal response uniformity, minimum achievable counting window width, maximum count rate, and system thermal stability.

### A. Counting window

In order to test the uniformity of the counting window and its minimum and maximum widths, we picked up the output stage signal (before the CPLD) and fed it to the START input of a TCSPC board (SPC-630 by Becker and Hickl GmbH, Germany). A pulse generator (81150A by Agilent Technologies, USA) was set to 5 MHz and the output was fed both to the STOP input of the TCSPC board and to the SYNC input of the gated counter under test. Finally, we connected a SPAD module in free-running mode (PDM by Micro Photon Devices Srl, Italy) to the PHOTON IN input of the gated counter. In this way, under ambient light illumination, the SPAD module provides a uniform distribution of pulses in time, uncorrelated with the 5 MHz pulse generator. Results are shown in Fig. 6. The left plot (Fig. 6(a)) shows the minimum

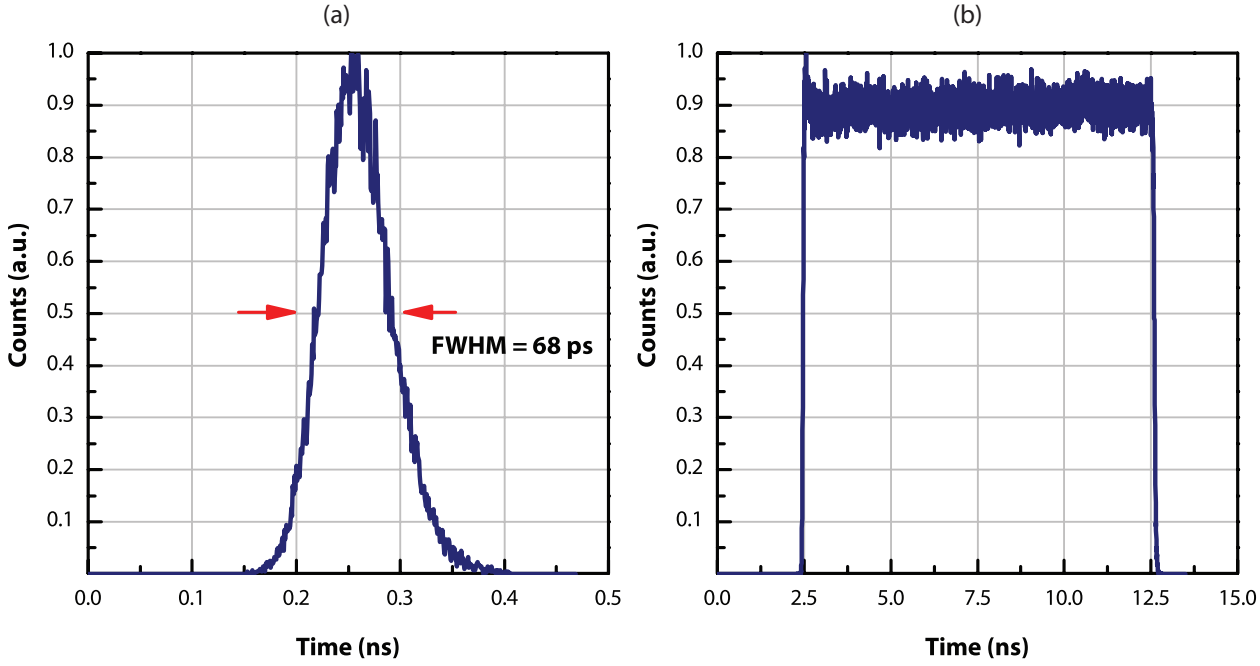


FIG. 6. Minimum (a) and maximum (b) detection windows obtainable with the gated photon counter. The minimum window width is 68 ps full-width at half maximum (FWHM) while the maximum window is 10 ns wide. The user can select any detection window in this range, with a fine resolution of 10 ps.

achievable window with a FWHM of 68 ps (which is not limited by the intrinsic timing jitter of the TCSPC board, i.e., about 8 ps). Figure 6(b) shows the maximum gate width of 10 ns FWHM, again with very sharp rising and falling edges (<35 ps, 20%–80%) and a flat, uniform temporal response.

### B. Maximum count rate

In order to measure the maximum achievable count rate and assess accuracy at different count rates and integration times, we connected the gated photon counter in parallel with a reference counter (53131A by Agilent Technologies, USA). The output of a pulse generator (81150A by Agilent Technologies, USA) has been split in two and fed to both SYNC and PHOTON IN inputs. Both counting windows have been set to 10 ns widths and to be coincident with the incoming PHOTON IN pulses, in order to count every generated pulse. The same signal was connected to the commercial counter to provide a reference count value, with an accuracy of less than 5 ppm. Table I shows the obtained results. The maximum achievable count rate is 100 Mcps with an error of 5.6 ppm with respect to the reference value at 10 s integration time.

The limitation in the maximum count rate is set by the used CPLD, which offers a wide range of functionalities but has a minimum pulse width of 8 ns. The good accuracy is obtained, thanks to the crystal oscillator employed as time base for the integration time, which shows a maximum frequency error of 25 ppm over a temperature range of 80 °C.

### C. Thermal stability

The internal components of the gated photon counter are sensitive to thermal drifts, especially the programmable delay lines used to synchronize signals and to select the counting window widths. The delay line data-sheet reports a worst-case temperature sensitivity of 15 ps/°C, which is comparable with the window transition times and therefore should be compensated to avoid drifts in the measured data. To ensure proper operation of the module and a long-term stability, an adequate thermal stabilization is needed. We used only passive solutions: a copper heat sink, placed on the bottom of the PCB, connects together the sensitive components to the aluminum box and a fan provides proper heat exchange. Moreover, both PHOTON IN and SYNC signals have identical path lengths in the layout and pass through the same number and type of components in order to minimize the effect of common-mode thermal drifts between the two signals.

Figure 7 shows an estimate of the capability of the thermal stabilization system. In Fig. 7(a) a 1 MHz square-wave signal is applied to both PHOTON IN and SYNC inputs and is placed just on the edge of the counting window, at 80%

TABLE I. Count rate error in parts per million (ppm) at different integration times (in seconds).

| Input count rate | Error at 0.1 s (ppm) | Error at 1 s (ppm) | Error at 10 s (ppm) |
|---|---|---|---|
| 10 Hz | <1 | <1 | <1 |
| 100 Hz | <1 | <1 | <1 |
| 1 kHz | <1 | <1 | <1 |
| 10 kHz | <1 | <1 | <1 |
| 100 kHz | <1 | <1 | 4 |
| 1 MHz | <1 | 2.7 | 3.85 |
| 10 MHz | 3 | 2.91 | 3.94 |
| 100 MHz | 3.12 | 4.3 | 5.6 |

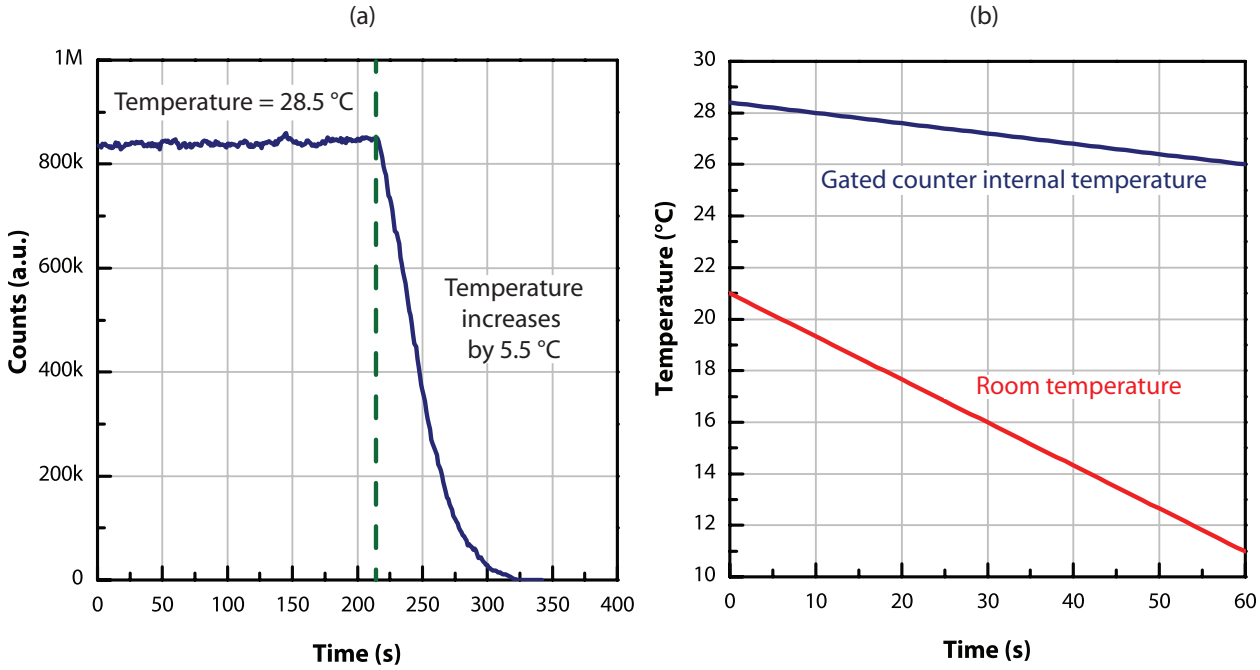


FIG. 7. (a) Count rate drift due to a temperature step increase. The counting window was set to 10 ns and 1 MHz input signal was integrated for 1 s. The input signal was synchronized at approximately 80% of the rising edge of the gating windows in order to obtain an 80% probability to detect every count (given a uniform distribution function of the detection probability) and to be extremely sensitive to time drifts. Following a +5.5 °C temperature step, the gating windows drifts in time (13 ps/°C) and the count rate drops to zero. (b) Temperature drift of the module's PCB versus environment temperature drift.

of the rising edge of one counting window, in order to have 80% probability to be detected at every trial (given a uniform distribution function of the detection probability). While the temperature is kept stable and uniform all over the board at 28.5 °C by the passive heat sink and the fan, the total counts integrated for 1 s are stable and correspond to approximately 800 kcps. By increasing the temperature with no temperature stabilization (i.e., removing the heat sink and the fan), the counting window position drifts (the delay of the counting window increases) and so the acquired counts drop to zero. Since the rise-time of the gate shaper is 35 ps (20%–80%) and the minimum temperature step to have zero counts is 5.5 °C, we estimated a drift of 13 ps/°C.

The passive solutions for temperature stabilization of the gated photon counter are enough to withstand the sudden ambient temperature changes of few celsius degrees that could happen during data acquisition. Figure 7(b) shows the temperature drift of the PCB during an abrupt ambient temperature change: for a 10 °C change in room temperature in 60 s, the internal temperature of the module changes by only 2 °C, thus limiting the overall counting window drift during data acquisition. If the ambient temperature does not recover to the initial value, also the gated photon counter temperature will reach the new asymptotic value, but with a very long time constant. Only an active temperature stabilization solution (like a thermo-electric cooler) would compensate such drift.

### D. Life-time measurements

Figure 8 shows the time response of a commercial silicon SPAD detector (PDM by Micro Photon Devices Srl, Italy) to a picosecond pulsed laser (40 MHz pulse repetition frequency, $\lambda = 670$ nm, FWHM = 100 ps, PDL-800 by Picoquant GmbH, Germany), reconstructed with three different techniques. The blue solid line (bottom) is the waveform acquired with a classical TCSPC board (SPC-630 by Becker and Hickl GmbH, Germany): the SPAD response exhibits a typical exponential diffusion tail[25] with a measured time constant of 258 ps.

In order to show the functionality of the gated counter, a 5 s acquisition of the SPAD response was performed with two counting windows (80 ps width) placed along the exponential tail and spaced 1 ns apart. The two black diamond markers represent the integrated counts $N_1$ and $N_2$ in the two windows at time $t_1$ and $t_2$. By knowing *a priori* that the waveform can be described by an exponential function N(t):

$$N(t) = A \times e^{-t/\tau_D}, \tag{1}$$

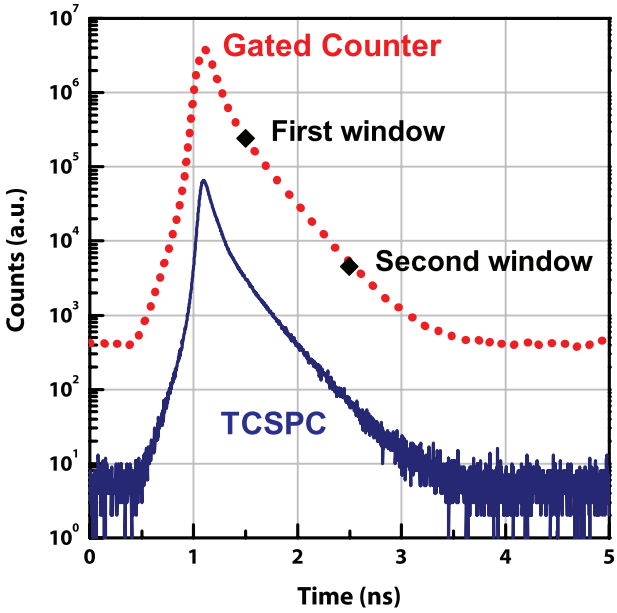


FIG. 8. Temporal response of a silicon SPAD to a picosecond laser pulse at 670 nm with 40 MHz repetition rate. The typical exponential decay (258 ps time-constant) is reconstructed with a TCSPC board (blue line), with the gated counter by shifting a single 80 ps window at 10 ps steps (red dots) and can also be computed with a simple two windows acquisition (diamond markers).

the time constant $\tau$ can be extracted with the following formula:

$$\tau_D = \frac{t_2 - t_1}{\ln(N_1/N_2)}, \tag{2}$$

where $\tau_D$ turns out to be 251 ps, in good agreement with the value estimated by the TCSPC board.

It is important to note that the proposed gated counter is not just a two-point counter. In fact it can also be exploited to reconstruct the entire time-dependent optical waveform. The red dotted curve (top) in Fig. 8 shows the same temporal response reconstructed with the gated photon counter, by shifting an 80 ps window at 10 ps steps with respect to the laser SYNC signal and integrating the collected counts for 5 s at each step. The time-constant in this case turns out to be 267 ps.

Thanks to its two very sharp (<70 ps) counting windows and precise timing management (the jitter of each components is <1 ps), we demonstrated that the developed gated photon counter is able to extract with good accuracy (<5%) information about a fast optical waveform with no need to

TABLE II. Comparison of the performance of the gated photon counter presented in this work and state-of-the-art alternatives.

| | Channels | Gates per channel | Acquisition rate (Mcps) | Counter depth (bit) | Mininum gate width (ns) | Integrated detector |
|---|---|---|---|---|---|---|
| This work | 1 | 2 | 100 | 32 | 0.07 | No |
| Becker and Hickl GmbH[20] | 2 | 1 | 800 | 32 | 1 | No |
| Stanford Research Systems[21] | 2 | 1 | 200 | 32 | 5 | No |
| Stoppa *et al.*[22] | 14 | 1 | 1 | 17 | 0.5 | CMOS SPAD |
| Rae *et al.*[23] | 64 | 2 | 4 | 9 | 0.41 | CMOS SPAD |

use any hardware or software demanding techniques, like TCSPC.

## IV. CONCLUSION

We presented the design and characterization of a high-throughput gated photon counter, able to count electrical signals within two well-defined and programmable detection windows. The module has a user-friendly interface and is fully programmable via a USB link by a remote computer. The performances of the whole instrument are summarized in Table II, where the proposed module is compared with other commercial and research products.

The design is also easily parallelizable both in integrated circuits, programmable (CPLD or Field Programmable Logic Array, FPGA) logics, or discrete component designs, when cost-effective, compact, and high-throughput multichannel acquisition systems must be developed. Therefore, it is suitable for many applications such as fluorescence lifetime imaging, Förster resonance energy transfer, fluorescence correlation spectroscopy, functional brain imaging, optical mammography, molecular imaging, quantum information, and many others, as a cost-effective alternative to TCSPC equipment.

[1]W. Becker, A. Bergmann, M. A. Hink, K. Konig, K. Benndorf, and C. Biskup, Microsc. Res. Tech. **63**, 58 (2004).
[2]W. Becker, A. Bergmann, and C. Biskup, Microsc. Res. Tech. **70**, 403 (2007).
[3]C. Biskup, T. Zimmer, L. Kelbauskas, B. Hoffmann, N. Klocker, W. Becker, A. Bergmann, and K. Benndorf, Microsc. Res. Tech. **70**, 442 (2007).
[4]W. Becker, K. Benndorf, A. Bergmann, C. Biskup, K. Konig, U. Tirlapur, and T. Zimmer, Proc. SPIE **4431**, 94 (2001).
[5]S. T. Hess, S. Huang, A. A. Heikal, and W. W. Webb, Biochem. **41**(3), 697 (2002).
[6]J. Selb, J. J. Stott, M. A. Franceschini, A. G. Sorensen, and D. A. Boas, J. Biom. Opt. **10**(1), 011013 (2005).
[7]A. Pifferi, A. Farina, A. Torricelli, G. Quarto, R. Cubeddu, and P. Taroni, J. Near Infrared Spectrosc. **20**(1), 223 (2012).
[8]K. Vishwanath, B. Pogue, and M. A. Mycek, Phys. Med. Biol. **47**(18), 3387 (2002).
[9]W. Becker, *Advanced Time-Correlated Single Photon Counting Techniques* (Springer, Berlin, 2005).
[10]A. Pifferi, A. Torricelli, L. Spinelli, D. Contini, R. Cubeddu, F. Martelli, G. Zaccanti, A. Tosi, A. Dalla Mora, F. Zappa, and S. Cova, Phys. Rev. Lett. **100**(13), 138101 (2008).
[11]Becker and Hickl GmbH, SPC-130 data-sheet, see http://www.becker-hickl.de/.
[12]PicoQuant GmbH, PicoHarp 300 data-sheet, see http://www.picoquant.com/.
[13]B. Markovic, S. Tisa, F. A. Villa, A. Tosi, and F. Zappa, IEEE Trans. Circuits Syst. I **60**(3), 557 (2013).
[14]M. Crotti, I. Rech, and M. Ghioni, IEEE J. Solid-State Circ. **47**(3), 699 (2012).
[15]G. Brida, I. P. Degiovanni, V. Schettini, S. V. Polyakov, and A. Migdall, J. Mod. Opt. **56**(2), 405 (2009).
[16]A. Restelli, J. C. Bienfang, and A. L. Migdall, J. Mod. Opt. **59**, 1465 (2012).
[17]N. Namekata, S. Adachi, and S. Inoue, IEEE Photon. Technol. Lett. **22**, 529 (2010).
[18]K. A. Patel, J. F. Dynes, A. W. Yuan, R. V. Penty, and A. J. Shields, Electron. Lett. **48**(2), 111 (2012).
[19]G. N. Gol'tsman, O. Okunev, G. Chulkova, A. Lipatov, A. Semenov, K. Smirnov, B. Voronov, A. Dzardanov, C. Williams, and R. Sonolwski, Appl. Phys. Lett. **79**(6), 705 (2001).
[20]Becker and Hickl GmbH, PMS-400A data-sheet, see http://www.becker-hickl.de/.
[21]Stanford Research Systems, SR-400 data-sheet, see http://www.thinksrs.com.
[22]D. Stoppa, D. Mosconi, L. Pancheri, and L. Gonzo, IEEE Sens. J. **9**(9), 1084 (2009).
[23]B. R. Rae, K. R. Muir, Z. Gong, J. McKendry, J. M. Girkin, E. Gu, D. Renshaw, M. Dawson, and R. K. Henderson, Sensors **9**, 9255 (2009).
[24]F. Zappa, S. Tisa, A. Tosi, and S. Cova, Sens. Actuators A **140**(1), 103 (2007).
[25]M. Ghioni, A. Gulinatti, I. Rech, F. Zappa, and S. Cova, IEEE J. Sel. Top. Quantum Electron. **13**(4), 852 (2007).